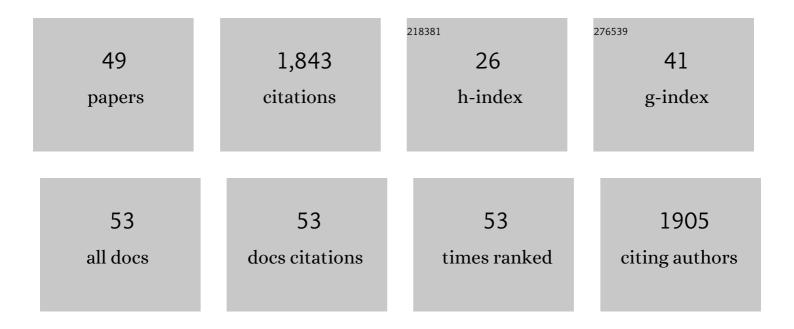
## Hassan Ait ahsaine

List of Publications by Year in descending order

Source: https://exaly.com/author-pdf/6426451/publications.pdf Version: 2024-02-01



#	Article	IF	CITATIONS
1	Recent progress on the synthesis, morphology and photocatalytic dye degradation of BiVO <sub>4</sub> photocatalysts: A review. Catalysis Reviews - Science and Engineering, 2024, 66, 214-258.	5.7	49
2	Synthesis, structural and the corrosion inhibition of phosphate-based xPbO–yB2O3–zP2O5 glass for C35 steel in acidic media. Nanotechnology for Environmental Engineering, 2022, 7, 277-287.	2.0	1
3	CO2 Electroreduction over Metallic Oxide, Carbon-Based, and Molecular Catalysts: A Mini-Review of the Current Advances. Catalysts, 2022, 12, 450.	1.6	14
4	Photocatalytic activity of anatase-brookite TiO2 nanoparticles synthesized by sol gel method at low temperature. Optical Materials, 2022, 129, 112256.	1.7	35
5	Removal of reactive red-198 dye using chitosan as an adsorbent: optimization by Central composite design coupled with response surface methodology. Toxin Reviews, 2021, 40, 225-237.	1.5	22
6	Synthesis and luminescence spectroscopy study of a novel orangeâ€red colour emissions phosphor based on Tb <sup>3+</sup> ionâ€doped Na <sub>2</sub> ZnP <sub>2</sub> O <sub>7</sub> . Luminescence, 2021, 36, 489-496.	1.5	5
7	Operando Elucidation on the Working State of Immobilized Fluorinated Iron Porphyrin for Selective Aqueous Electroreduction of CO <sub>2</sub> to CO. ACS Catalysis, 2021, 11, 6499-6509.	5.5	27
8	Recent trends on numerical investigations of response surface methodology for pollutants adsorption onto activated carbon materials: A review. Critical Reviews in Environmental Science and Technology, 2020, 50, 1043-1084.	6.6	109
9	Experimental Investigation of the Effects of Synthesis Parameters on the Precipitation of Calcium Carbonate and Portlandite from Moroccan Phosphogypsum and Pure Gypsum Using Carbonation Route. Waste and Biomass Valorization, 2020, 11, 6953-6965.	1.8	20
10	New amino group functionalized porous carbon for strong chelation ability towards toxic heavy metals. RSC Advances, 2020, 10, 31087-31100.	1.7	20
11	Nitrogen doped graphitic porous carbon from almond shells as an efficient persulfate activator for organic compound degradation. New Journal of Chemistry, 2020, 44, 9391-9401.	1.4	17
12	Microwave assisted green synthesis of Fe <sub>2</sub> O <sub>3</sub> /biochar for ultrasonic removal of nonsteroidal anti-inflammatory pharmaceuticals. RSC Advances, 2020, 10, 11371-11380.	1.7	37
13	UV-light photocatalytic properties of the bismuth lutetium tungstate system Bi2-xLuxWO6 (0Ââ‰ÂxÂâ‰Â1). Materials Letters, 2020, 276, 128221.	1.3	14
14	The Growth of Photoactive Porphyrin-Based MOF Thin Films Using the Liquid-Phase Epitaxy Approach and their Optoelectronic Properties. Materials, 2019, 12, 2457.	1.3	11
15	High extent mass recovery of alginate hydrogel beads network based on immobilized bio-sourced porous carbon@Fe3O4-NPs for organic pollutants uptake. Chemosphere, 2019, 236, 124351.	4.2	43
16	Kinetics, equilibrium, statistical surface modeling and cost analysis of paraquat removal from aqueous solution using carbonated jujube seed. RSC Advances, 2019, 9, 1084-1094.	1.7	43
17	Combined Methane Energy Recovery and Toxic Dye Removal by Porous Carbon Derived from Anaerobically Modified Digestate. ACS Omega, 2019, 4, 9434-9445.	1.6	31
18	Compositionally Screened Eutectic Catalytic Coatings on Halide Perovskite Photocathodes for Photoassisted Selective CO <sub>2</sub> Reduction_ACS Energy Letters_2019_4_1279-1286	8.8	56

HASSAN AIT AHSAINE

#	Article	IF	CITATIONS
19	Carbon microspheres derived from walnut shell: Rapid and remarkable uptake of heavy metal ions, molecular computational study and surface modeling. Chemosphere, 2019, 231, 140-150.	4.2	42
20	Preparation and Characterization of Porous Carbon@ZnOâ€NPs for Organic Compounds Removal: Classical Adsorption Versus Ultrasound Assisted Adsorption. ChemistrySelect, 2019, 4, 4981-4994.	0.7	30
21	Selected pharmaceuticals removal using algae derived porous carbon: experimental, modeling and DFT theoretical insights. RSC Advances, 2019, 9, 9792-9808.	1.7	48
22	Electrosynthesis of zinc phosphate-polypyrrole coatings for improved corrosion resistance of steel. Surfaces and Interfaces, 2019, 15, 224-231.	1.5	34
23	Reusable bentonite clay: modelling and optimization of hazardous lead and <i>p</i> -nitrophenol adsorption using a response surface methodology approach. RSC Advances, 2019, 9, 5756-5769.	1.7	35
24	Carbonaceous material prepared by ultrasonic assisted pyrolysis from algae (Bifurcaria bifurcata): Response surface modeling of aspirin removal. Surfaces and Interfaces, 2019, 14, 61-71.	1.5	25
25	Cationic dyes adsorption onto high surface area â€~almond shell' activated carbon: Kinetics, equilibrium isotherms and surface statistical modeling. Materials Today Chemistry, 2018, 8, 121-132.	1.7	141
26	Well-designed WO <sub>3</sub> /Activated carbon composite for Rhodamine B Removal: Synthesis, characterization, and modeling using response surface methodology. Fullerenes Nanotubes and Carbon Nanostructures, 2018, 26, 389-397.	1.0	53
27	Facile synthesis, characterization and photocatalytic performance of Zn3(PO4)2 platelets toward photodegradation of Rhodamine B dye. Journal of Environmental Chemical Engineering, 2018, 6, 1840-1847.	3.3	72
28	Acridine orange adsorption by zinc oxide/almond shell activated carbon composite: Operational factors, mechanism and performance optimization using central composite design and surface modeling. Journal of Environmental Management, 2018, 206, 383-397.	3.8	115
29	Adsorptive Removal of Methylene Blue and Crystal Violet onto Micro-Mesoporous Zr <sub>3</sub> O/Activated Carbon Composite: A Joint Experimental and Statistical Modeling Considerations. Journal of Chemistry, 2018, 2018, 1-14.	0.9	36
30	Apatitic tricalcium phosphate powder: High sorption capacity of hexavalent chromium removal. Surfaces and Interfaces, 2018, 13, 139-147.	1.5	31
31	Photo/Electrocatalytic Properties of Nanocrystalline ZnO and La–Doped ZnO: Combined DFT Fundamental Semiconducting Properties and Experimental Study. ChemistrySelect, 2018, 3, 7778-7791.	0.7	34
32	Porous carbon by microwave assisted pyrolysis: An effective and low-cost adsorbent for sulfamethoxazole adsorption and optimization using response surface methodology. Journal of Cleaner Production, 2018, 202, 571-581.	4.6	108
33	Adsorption kinetics and surface modeling of aqueous methylene blue onto activated carbonaceous wood sawdust. Fullerenes Nanotubes and Carbon Nanostructures, 2018, 26, 433-442.	1.0	42
34	Electrical impedance spectroscopy analyses and optical properties of the bismuth lutetium tungstate BiLuWO <sub>6</sub> . Ferroelectrics, 2017, 515, 112-119.	0.3	1
35	Bismuth Silver Oxysulfide for Photoconversion Applications: Structural and Optoelectronic Properties. Chemistry of Materials, 2017, 29, 8679-8689.	3.2	28
36	Effects of lutetium doping on the X-ray-excited luminescence properties of theÂtungstate Zn1â^'x Lu x WO4. Research on Chemical Intermediates, 2017, 43, 885-899.	1.3	0

HASSAN AIT AHSAINE

#	Article	IF	CITATIONS
37	Electrocatalytic properties of hydroxyapatite thin films electrodeposited on stainless steel substrates. Mediterranean Journal of Chemistry, 2017, 6, 255-266.	0.3	21
38	MAPbl2.9-xBrxCl0.1 hybrid halide perovskites: Shedding light on the effect of chloride and bromide ions on structural and photoluminescence properties. Applied Surface Science, 2016, 390, 744-750.	3.1	16
39	Electronic band structure and visible-light photocatalytic activity of Bi <sub>2</sub> WO <sub>6</sub> : elucidating the effect of lutetium doping. RSC Advances, 2016, 6, 101105-101114.	1.7	57
40	Congo red removal by PANi/Bi2WO6 nanocomposites: Kinetic, equilibrium and thermodynamic studies. Journal of Environmental Chemical Engineering, 2016, 4, 3096-3105.	3.3	51
41	Novel Lu-doped Bi2WO6 nanosheets: Synthesis, growth mechanisms and enhanced photocatalytic activity under UV-light irradiation. Ceramics International, 2016, 42, 8552-8558.	2.3	53
42	Role of the chemical substitution on the structural and luminescence properties of the mixed halide perovskite thin MAPbI3â^'xBrx (O ≤ ≤) films. Applied Surface Science, 2016, 371, 112-117.	3.1	98
43	Novel synthesis, characterization and optical properties of Lu2O3 deposited by electrochemical method. Materials Letters, 2015, 160, 415-418.	1.3	7
44	Structural, vibrational study and UV photoluminescence properties of the system Bi <sub>(2â^'x)</sub> Lu <sub>(x)</sub> WO <sub>6</sub> (0.1 ≤ ≤). RSC Advances, 2015, 5, 96242-962	52: <sup>7</sup>	18
45	Rietveld refinements, impedance spectroscopy and phase transition of the polycrystalline ZnMoO4 ceramics. Ceramics International, 2015, 41, 15193-15201.	2.3	28
46	Structural, microstructural and vibrational analyses of the monoclinic tungstate BiLuWO6. Journal of Solid State Chemistry, 2014, 218, 124-130.	1.4	12
47	Electron microscopy analyses and electrical properties of the layered Bi2WO6 phase. Journal of Solid State Chemistry, 2013, 203, 8-18.	1.4	15
48	Mesoporous treated sewage sludge as outstanding low-cost adsorbent for cadmium removal. , 0, 85, 330-338.		33
49	Fabrication, characterization and competitive study of toxic dyes adsorption onto Mg3Al-CO32â^' clay adsorbent. Nanotechnology for Environmental Engineering, 0, , 1.	2.0	0